Available online at www.sciencedirect.com
ScienceDirect
Computers and Structures 86 (2008) 1417–1425
Computers & Structures
www.elsevier.com/locate/compstruc

Optimum structure with homogeneous optimum truss-like material

Ling Liu *,[1], Jun Yan, Gengdong Cheng *

State Key Laboratory of Structural Analysis for Industrial Equipment, Department of Engineering Mechanics, Dalian University of Technology, Dalian 116024, PR China

Received 5 March 2007; accepted 30 April 2007
Available online 24 March 2008

Abstract

This paper presents a concurrent topology optimization method to simultaneously achieve the optimum structure and material microstructure for minimum system compliance. Microstructure is assumed to be uniform in macro-scale to meet manufacturing requirements. Design variables for structure and material microstructure are independently defined and then integrated into one system with the help of homogenization theory. Penalization approaches are adopted in both scales to ensure clear topologies, i.e. SIMP (Solid Isotropic Material with Penalization) in micro-scale and PAMP (Porous Anisotropic Material with Penalization) in macro-scale. Numerical experiments for two examples validate the proposed method and also demonstrate the superiority of truss-like materials.

Keywords: Ultra-light material; Microstructure; Homogenization; Topology optimization; Concurrent optimization

1. Introduction

Proposed in the late 20th century, ultra-light materials mostly refer to porous and structured materials including foam [1], truss-like material [2] and linear cellular material [3,4]. These kinds of materials are widespread in natural world and very promising in practical applications because of their relatively high stiffness/strength – weight ratios and tremendous opportunity for multifunctional applications. And compared with traditional advanced materials such as fiber-reinforced and particle-reinforced composites, they are superior in being free from interface problem and high anisotropy.

The ultra-light materials can be divided into two groups. The first one is represented by foam material that has intrinsic microscopic randomness in microstructures. Another group, including truss-like material [10] and linear cellular material as shown in Fig. 1, differentiates itself by microstructures distributed periodically in space. The latter ones also have two additional strengths, namely their perfect periodicity and high designability. The increasing recognition of this designability, along with the rapid developments in fabrication techniques [5–7], has made it particularly meaningful and applicable to design structures made of porous anisotropic materials.

Ultra-light structure is always a hot topic in automobile, aerospace and aircraft industries which is able to reduce structural weight and energy consumption, and thereby greatly improve the quality of products. In the meantime, ultra-light materials are desirable in designing ultra-light structures due to their superior properties and multifunctional capability. The present paper is, therefore, an attempt to design ultra-light structures composed of ultra-light materials for minimum compliance, and topology optimization is utilized as a key tool.

Structural topology optimization aims at finding optimum topology to minimize structural weight or maximize structural performance for a given set of constraints. In comparison with size and shape optimization, topology optimization results in more efficient design and may generate the optimum conception/configuration required in the stage of initial design. The pioneering work of modern

* Corresponding authors.
E-mail addresses: ll2405@columbia.edu (L. Liu), chenggd@dlut.edu.cn (G. Cheng).
[1] Current address: Department of Civil Engineering and Engineering Mechanics, Columbia University, New York, NY 10027-6699, USA.

0045-7949/$ - see front matter © 2008 Elsevier Ltd. All rights reserved.
doi:10.1016/j.compstruc.2007.04.030

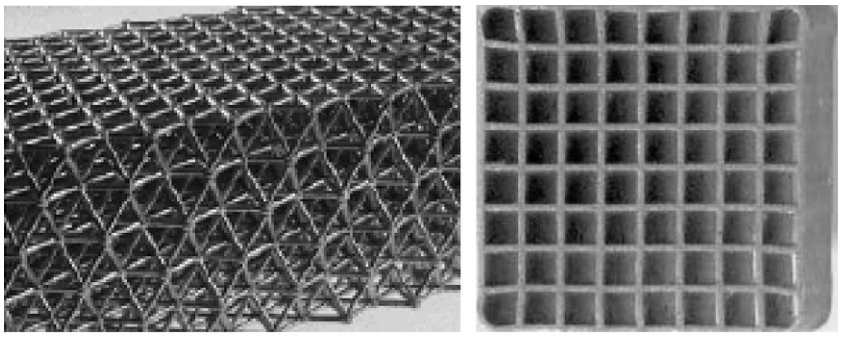

Truss-like material[10] Linear cellular material[4]

Fig. 1. Two representations of ultra-light materials.

structural topology optimization can be traced back to 1981, when Cheng and Olhoff [8] introduced the concept of microstructure to structural optimization in studying the optimum thickness design of a solid elastic plate for minimum compliance. In 1988, Bendsoe and Kikuchi [9] implemented the topology optimization via a homogenization method. In their work, design domain is assumed to be porous material consisting of infinite number of cells. Each cell contains solid material plus an internal cavity, which is commonly assumed to be some specific configurations parameterized by one or more variables chosen as design variables. Then by size optimization, material is redistributed in the design domain. Cells with large cavities (and hence low material density) will be treated as void while those with small cavities (and large material density) denote solid part and form the structure.

An alternative, but conceptually similar approach to implement structural topology optimization is the so-called SIMP (Solid Isotropic Material with Penalization) method [11]. Densities of elements are set as design variables for interpolating between solid material and void. Region with high density is identified as solid while region with low value is interpreted as void. Relationship between the design variable and the material properties is established based on a power law, which is simple and artificial but pretty effective.

Application of the above two approaches often leads to structural design containing gray area, which is neither solid nor void. In the homogenization-based approach, gray area consists of cells with cavities of intermediate size. They do resemble certain composite materials with microstructures, but the material microstructures vary pointwise, which can be hardly manufactured. In SIMP approach, the gray area has material density between zero and one. Certain microstructures were proposed to match those materials with intermediate densities in the sense of effective elastic properties [12].

To achieve clear "black–white" topology, researchers have developed various penalty methods [12] to avoid generation of gray elements, or presence of material with complicated microstructures. This design concept is being challenged when ultra-light materials are increasingly applied in engineering, for which, macro relative density is no longer 1 but an intermediate value between 0 and 1. Rodrigues et al. [13] in 2002 proposed a hieratical design of structure and material. The work strongly underlines optimization of material microstructures and some reasonably good results have been achieved. However, microstructural configuration varies considerably from point to point in macro-scale, which results in a "varying gray" look of the structural design. Such results may give rise to an insurmountable manufacturing difficulty.

The present work is an attempt to achieve ultra-light structures composed of ultra-light materials by utilizing topology optimization in both structural and material scales. To improve the possibility of practical applications, manufacturing factors are strongly underlined by assuming the uniformity of material microstructures in macro-scale.

The design of material microstructure is independently defined in our work and concurrently performed with the structural design. In topology optimization implemented by homogenization, however, microstructure is involved in the design process but the design in micro-scale is merely limited to the scope of size optimization with the ultimate objective of structural topology optimization. And in SIMP, microstructure is introduced merely for validating the material interpolation model, but not integrated into the design process.

The concurrent design confers a great advantage in taking into account the interaction of both scales, which makes it distinct from those independent designs of material microstructures [14–18] aimed at developing materials with prescribed or extreme properties. Optimum material microstructure obtained by independent design is merely optimum in terms of equivalent properties, not ensured to be efficient when applied to constructing structures, since both structural configuration and boundary conditions are varied in practical use. In concurrent design of structures and materials, however, optimum structure and optimum material microstructure can simultaneously be obtained. That is to say, the resulting material microstructure is optimum for the optimum structure and the resulting structure is optimum for the optimum material microstructure. System performance, therefore, can be expected the best.

The organization of the rest of this paper is as follows. Mathematical model is given in Section 2, where two class design variables, i.e. macro density and micro density are

independently defined. Section 3 presents the penalization and numerical treatments aimed at obtaining clear topologies in both scales. Section 4 deals with the structural analysis and sensitivity analysis required for numerical optimization algorithms. And Section 5, finally, outlines two numerical examples in order to validate the proposed method and to discuss all the parameters involved in the formulation.

2. Problem statement

Fig. 2 illustrates a structure composed of a porous anisotropic material with uniform microstructures. There are two materials involved in our study, the base material and the porous anisotropic material. The base material could be any type of solid materials such as aluminum and alloy. Porous anisotropic material, sometimes merely called 'material' for short in the following discussions, is assumed to be made of the base material and to have periodic microstructure free from any restrictions (e.g. the cavities in linear cellular materials and ranked laminates are usually regularly shaped).

In this paper, we are trying to obtain neither "black–white" design nor "varying gray" design. Our objective is to find a "gray–white" design as shown in Fig. 2 with maximized system performance by emphasizing the uniformity of the "grey level", i.e. material relative density, in macro-scale. Here arise two basic problems:

1. Micro-scale: How to interpret the "gray" material? As stated before, porous material can be characterized by certain periodic microstructure. So one of the major objectives is to design the material over its smallest representative unit, i.e. a unit cell (or base cell) Y.
2. Macro-scale: How to arrange the "gray" material? Problem in this scale lies in the optimum distribution of the porous material with optimized microstructure.

Both problems can be dealt with as classical layout designs, for which topology optimization is a powerful tool. Two classes of design variables are independently defined, i.e. macro density $\mathbf{P}(\mathbf{X})$ in structural design domain and micro density $\rho(\mathbf{Y})$ in a unit cell, both ranging from 0 to 1. Assuming optimum structural design is imbedded in the design domain Ω and is subject to external load F, the minimum compliance design can therefore be formulated as

$$\text{Minimize}: C = \int_{\Omega} F \cdot U \, \mathrm{d}\Omega \tag{1}$$

$$\text{Constraint I}: \varsigma = \frac{\rho^{\mathrm{PAM}} \cdot \int_{\Omega} P \, \mathrm{d}\Omega}{V^{\mathrm{MA}}} \leqslant \bar{\varsigma} \tag{2}$$

$$\text{Constraint II}: \rho^{\mathrm{PAM}} = \frac{\int_{Y} \rho \, \mathrm{d}Y}{V^{\mathrm{MI}}} = \overline{\overline{\varsigma^{\mathrm{MI}}}} \tag{3}$$

$$\text{Constraint III}: 0 < \delta \leqslant P \leqslant 1, \quad 0 < \delta \leqslant \rho \leqslant 1 \tag{4}$$

where C denotes structural compliance and U represents structural deformation dependent on the densities in both scales.

Constraint I sets an upper bound on the total available base material by defining relative volume ς smaller than a prescribed value $\bar{\varsigma}$. V^{MA} is the area of macro design domain Ω. Due to the use of porous material, the definition of ς is somewhat different form that in general formulation of single-scaled topology optimization. ρ^{PAM}, relative density of the porous anisotropic material, is included here. But in single-scaled topology optimization, the relative density should equal to 1.

Constraint II makes ρ^{PAM} equal to a given value $\overline{\overline{\varsigma^{\mathrm{MI}}}}$, which should be between 0.2 and 0.6 according to practical fabrication techniques. By defining this equality constraint, the material is ensured to be porous with a given relative density.

By virtue of Constraints (2) and (3), the consumption of porous anisotropic material in macro-scale can thereby be predicted as follows:

$$\frac{\varsigma}{\rho^{\mathrm{PAM}}} = \frac{\int_{\Omega} P \, \mathrm{d}\Omega}{V^{\mathrm{MA}}} \leqslant \frac{\bar{\varsigma}}{\overline{\overline{\varsigma^{\mathrm{MI}}}}} \tag{5}$$

where ς and ρ^{PAM} denote the volume fraction filled with the base material in total and in the micro design domains, respectively. Therefore, their ratio in the left hand side of the inequality can be interpreted as the volume fraction occupied by the porous anisotropic material in the macro design domain, i.e. the consumption of the designed material in macro scale, on which the right hand side value imposes an upper bound. Given a constant $\bar{\varsigma}$, bigger $\overline{\overline{\varsigma^{\mathrm{MI}}}}$, i.e. more base material consumed in micro-scale design, will definitely lead to a stricter constraint for macro-scale design.

Constraint III sets bounds for density variables in two scales, where δ is a small predetermined value that is rather close to zero.

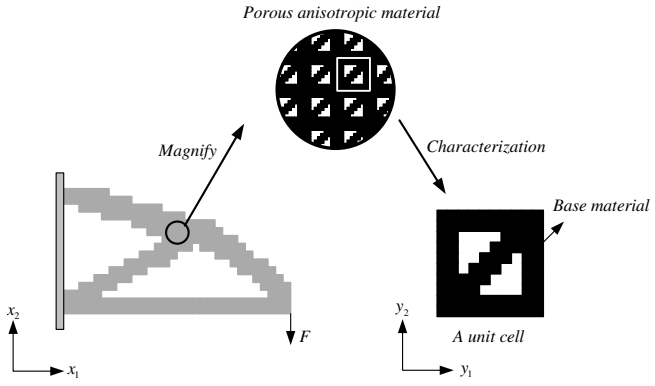

Fig. 2. A structure composed of porous anisotropic material.

3. Penalization and numerical treatments

To numerically solve the mathematical problem via FEM (Finite Element Method), computational domains in both scales should be first meshed into a number of elements. As shown in Fig. 3, domain Ω is meshed into N elements and domain Y is meshed into n elements. Each element is

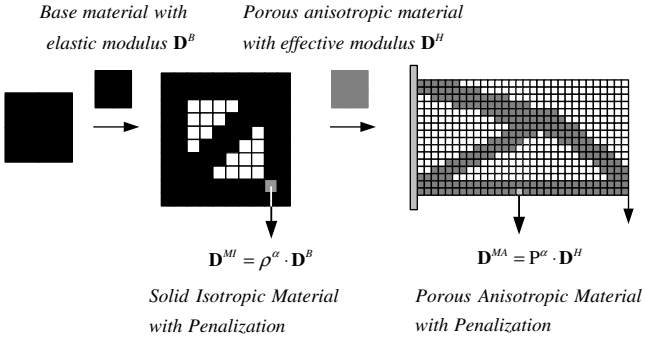

Fig. 3. Penalization-based concurrent optimization with two class design variables.

then assigned a unique density value varying between 0 and 1, e.g. P_i for the ith ($i = 1,2,\ldots,N$) element in macro-scale and ρ_j ($j = 1,2,\ldots,n$) for the jth element in micro-scale.

In order to achieve clear topologies in both scales, penalization methods are adopted. In micro-scale, it is natural to utilize SIMP (Solid Isotropic Material with Penalization), a method commonly used in some previous work of structural topology optimization. Assuming modulus matrix of the base material is $\mathbf{D}^B$, the modulus matrix at a point with density value ρ can be expressed as

$$\mathbf{D}^{\mathrm{MI}} = \rho^{\alpha} \cdot \mathbf{D}^B \tag{6}$$

where α denotes the exponent of penalization.

In macro-scale, however, it seems no longer appropriate to use SIMP because the material here is not guaranteed to be solid isotropic. In fact, since the design of microstructure follows topology optimization procedure and no restriction is ever imposed, the chance of getting porous anisotropic material is considerably high. As a result, we would like to name the macro-scale penalization as PAMP (Porous Anisotropic Material with Penalization), although the implementing process is remarkably similar to that of SIMP. Given any porous anisotropic material with modulus matrix $\mathbf{D}^{\mathrm{H}}$, a point with density P has the modulus matrix $\mathbf{D}^{\mathrm{MA}}$ as expressed by

$$\mathbf{D}^{\mathrm{MA}} = P^{\alpha} \cdot \mathbf{D}^{\mathrm{H}} \tag{7}$$

As will be indicated by numerical examples, only penalization is not enough for micro-scale design. Resulting microstructural topology can be very fuzzy if no further treatment is adopted. To limit the complexity of the admissible designs and to suppress the checkerboard pattern, a number of methods have been proposed such as: enforcing an upper bound on the perimeter of the structure [19], introducing a filtering function [16] and imposing constraints on the slope of the parameters defining the geometry [20]. In this paper, a variant perimeter constraint [21] will be utilized in micro-scale as the fourth constraint for the optimization problem.

$$\text{Constraint IV} : \gamma = \sum_{k=1}^{m} l_k \cdot (\rho_{k1} - \rho_{k2})^2 \leqslant \bar{\gamma} \tag{8}$$

where m denotes the number of element and l_k denotes the length of the kth interface between elements $k1$ and $k2$. $\bar{\gamma}$ is a predetermined upper bound. We will numerically discuss this parameter in Section 5.

4. Structural analysis and sensitivity analysis

It is a key step in numerical optimization to establish the relationship between objective function and design variables. According to Eq. (1), the designing objective, i.e. system compliance C in the present study, cannot be evaluated before the structural deformation U is solved. Finite element analysis is therefore formulated in macro-scale to obtain U as follows:

$$\mathbf{K} \cdot \mathbf{U} = \mathbf{F} \tag{9}$$

$$\mathbf{K} = \int_{\Omega} \mathbf{B}^{\mathrm{T}} \cdot \mathbf{D}^{\mathrm{MA}} \cdot \mathbf{B}\,\mathrm{d}\Omega \tag{10}$$

Here, $\mathbf{K}$ is stiffness matrix of the structure and $\mathbf{B}$ is the strain/displacement matrix. $\mathbf{U}$ and $\mathbf{F}$ are nodal values of U and F. $\mathbf{D}^{\mathrm{MA}}$ is defined in Eq. (7) as a function of $\mathbf{D}^{\mathrm{H}}$, which is to be determined by the following analysis.

$\mathbf{D}^{\mathrm{H}}$ serves as a crucial link between the two scales: on one hand it is a representation of effective material properties depending on microstructural configuration, and on the other it is also involved in macrostructural analysis as defined above. The computation of $\mathbf{D}^{\mathrm{H}}$ could follow the classical homogenization procedures by implementing the following two steps: Firstly, analyze the unit cell subjected to periodic boundary conditions and outer forces corresponding to uniform strain fields

$$\mathbf{k} \cdot \mathbf{u} = \int_{Y} \mathbf{b}^{\mathrm{T}} \cdot \mathbf{D}^{\mathrm{MI}}\,\mathrm{d}Y \tag{11}$$

$$\mathbf{k} = \int_{Y} \mathbf{b}^{\mathrm{T}} \cdot \mathbf{D}^{\mathrm{MI}} \cdot \mathbf{b}\,\mathrm{d}Y \tag{12}$$

where $\mathbf{k}$ is stiffness matrix of the microstructure, $\mathbf{u}$ is the microstructural deformation, $\mathbf{b}$ is the strain/displacement matrix and $\mathbf{D}^{\mathrm{MI}}$ is defined in Eq. (6).

Secondly, compute the effective modulus matrix by performing integration over the domain of a unit cell

$$\mathbf{D}^{\mathrm{H}} = \frac{1}{|Y|} \int_{Y} \mathbf{D}^{\mathrm{MI}} \cdot (\mathbf{I} - \mathbf{b} \cdot \mathbf{u})\,\mathrm{d}Y \tag{13}$$

where $\mathbf{I}$ (3×3) is a unit matrix in two-dimensional case and $|Y|$ is the area of a unit cell.

By virtue of Eqs. (6)–(13), we have completed the structural analysis in two scales and got the structural deformation $\mathbf{U}$. Following this procedure, one is able to evaluate the objective function C for any values of design variables.

A typical procedure of numerical optimization generally contains two major parts: the first one is ANALYSIS and another OPTIMUM SEARCH. For the latter one, a number of numerical methods are already available. In applying some derivative-based mathematical programming algorithms such as SLP (Sequential Linear Programming)

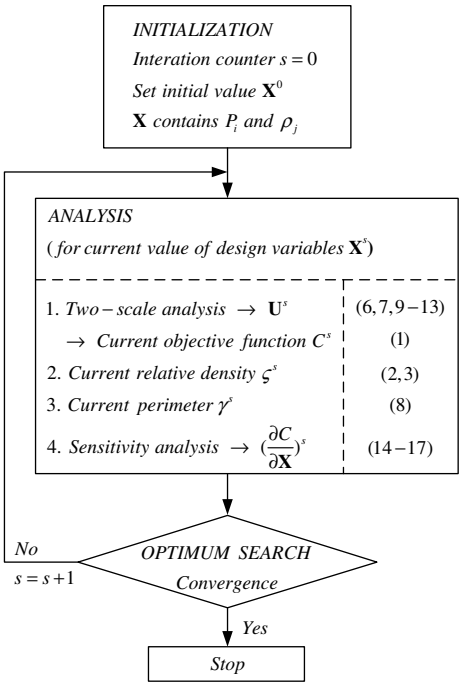

Fig. 4. Flow chart.

and SQP (Sequential Quadratic Programming), explicit expression of sensitivity is important to enhance the efficiency of the algorithm. By using all the above equations, it is readily to obtain the following two derivatives (see Appendix for details):

$$\frac{\partial C}{\partial P_i} = -\frac{\alpha \cdot C_i}{P_i} \tag{14}$$

$$\frac{\partial C}{\partial \rho_j} = -\sum_{r=1}^{N} P_r^{\alpha} \cdot \mathbf{U}_r^{\mathrm{T}} \cdot \left(\int_{\Omega_r} \mathbf{B}^{\mathrm{T}} \cdot \frac{\partial \mathbf{D}^{\mathrm{H}}}{\partial \rho_j} \cdot \mathbf{B}\, \mathrm{d}\Omega \right) \cdot \mathbf{U}_r \tag{15}$$

where the derivative of $\mathbf{D}^{\mathrm{H}}$ with respect to ρ_j can be computed following a mapping method [22] with the results as

$$\frac{\partial \mathbf{D}^{\mathrm{H}}}{\partial \rho_j} = \int_Y (\mathbf{I} - \mathbf{b} \cdot \mathbf{u})^{\mathrm{T}} \cdot \frac{\partial \mathbf{D}^{\mathrm{MI}}}{\partial \rho_j} \cdot (\mathbf{I} - \mathbf{b} \cdot \mathbf{u})\, \mathrm{d}Y \tag{16}$$

Combined with Eq. (6), the above equation leads to

$$\frac{\partial \mathbf{D}^{\mathrm{H}}}{\partial \rho_j} = \alpha \rho_j^{\alpha-1} \int_{Y_j} (\mathbf{I} - \mathbf{b} \cdot \mathbf{u}_j)^{\mathrm{T}} \cdot \mathbf{D}^{B} \cdot (\mathbf{I} - \mathbf{b} \cdot \mathbf{u}_j)\, \mathrm{d}Y \tag{17}$$

Now, we have completed the structural analysis and sensitivity analysis. A flow chart is given in Fig. 4 with each key step associated with corresponding equations.

5. Numerical examples and discussions

5.1. Numerical Example I: a discussion of parameters $\bar{\varsigma}$, $\overline{\overline{\varsigma^{\mathrm{MI}}}}$ and $\bar{\gamma}$

We first consider the so-called MBB beam. The main objective is both to illustrate the proposed method and to discuss the parameters $\bar{\varsigma}$, $\overline{\overline{\varsigma^{\mathrm{MI}}}}$ and $\bar{\gamma}$. As will be demonstrated, all of the three parameters do have an influence on the resulting topologies (structure and microstructure) and compliance. But they are different in nature: $\bar{\varsigma}$ and $\overline{\overline{\varsigma^{\mathrm{MI}}}}$ are involved in physical problem as limits of material consumption, while $\bar{\gamma}$ is merely a controlling parameter in numerical treatment.

A MBB beam in Fig. 5 is loaded with a concentrated vertical force of $P = 1000$ at the centre of the top edge and is supported on rollers at the bottom-right corner and on fixed supports at the bottom-left corner. Base material is assumed to have Young's modulus $E = 2.1 \times 10^5$ and Poisson's ratio $v = 0.3$. Geometric parameters are $L = 4$ and $h = 1$. As we are only interested in qualitative results, the dimensions and load for this problem are chosen non-dimensional. Due to the axial symmetry of the problem, only the right half part is considered as macro design domain. The mesh is 50×25 for macro design domain and 25×25 for the microstructure (8 Node Solid Element). OPTIMUM SEARCH is implemented by the optimization package DOT using the SQP algorithm.

To discuss the influence of the adopted perimeter constraint, the optimization problem is first solved with fixed $\bar{\varsigma} = 0.1$, $\overline{\overline{\varsigma^{\mathrm{MI}}}} = 0.4$ and varying perimeter constraint $\bar{\gamma}$. As shown in Table 1, if perimeter constraint is not applied

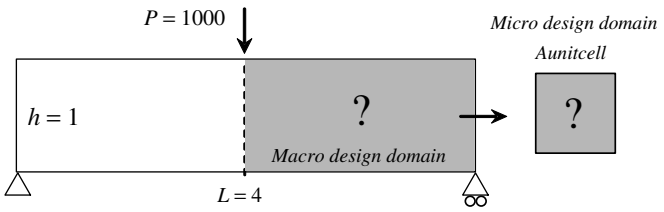

Fig. 5. MBB beam.

Table 1
Results for varying $\bar{\gamma}$

$\bar{\varsigma}$	$\overline{\overline{\varsigma^{\mathrm{MI}}}}$	$\bar{\gamma}$	Compliance	Microstructural topology
0.12	0.4	2	7515	
0.12	0.4	3	5675	
0.12	0.4	4	5676	
0.12	0.4	8	7077	
0.12	0.4	N/A	7583	

or controlling parameter is not small enough, the resulting microstructural topology tends be very complex, and the compliance value is relatively higher than those with appropriate $\bar{\gamma}$. So we suggest, partly based on the numerical results, that it is necessary to apply numerical treatments in micro-scale design to ensure a clear topology and better system performance. However, note that too small $\bar{\gamma}$ may lead to difficulties of convergence.

Then, we set $\bar{\gamma}$ to an appropriate value of 4 and solve the problem again with varying $\bar{\varsigma}$. As shown in Table 2, although resulting microstructures are all porous anisotropic, the topology does vary considerably for different conditions. When $\bar{\varsigma} = 0.25$, the microstructure after a rotation of 45° closely resembles the so-called 'Triangular cell' (see Fig. 6) which is said to have superior in-plane mechanical properties [3]. And when $\bar{\varsigma} = 0.075$, the microstructure after a rotation of 45° is somewhat more similar to the 'Mixed cell' (see Fig. 6), which is considered as another competitive microstructure for linear cellular material. These resemblances between our results and some existing superior microstructures imply the proposed method does generate microstructures with good equivalent properties. But they are not optimum if we only consider the equivalent properties. The reason is that the best system performance requires a microstructural topology best suiting the structural results, rather than those merely having extreme properties. In macro-scale, the design also changes with the increase of $\bar{\varsigma}$ in accordance with different material properties and changing available porous materials. As for the compliance value, it is reasonable that better system performance is achieved with more base material available.

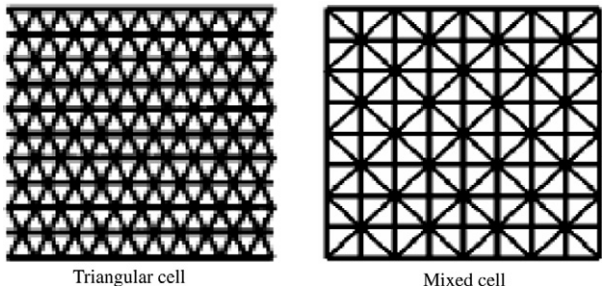

Fig. 6. Two microstructures for linear cellular material [3].

In Section 2, we have mentioned the trade-off between macro-scale design and micro-scale design, namely the allocation of material between the two scales which can be characterized by $\bar{\varsigma}/\overline{\overline{\varsigma^{MI}}}$ and $\overline{\overline{\varsigma^{MI}}}$. To illustrate the discussion, the two-scale design problem is solved again with predetermined available base material $\bar{\varsigma} = 0.12$ and varying $\overline{\overline{\varsigma^{MI}}}$. As shown in Table 3, larger value of $\overline{\overline{\varsigma^{MI}}}$ leads to lower system compliance with more base material consumption in micro-scale design and less porous material consumption in macro-scale design. That means in this case, it is advantageous to strengthen the porous material rather than enhancing the macrostructure. Does this conclusion hold for other examples or for other designing objectives? Further work is being carried out for exploring these questions.

Table 2
Results for varying $\bar{\varsigma}$

$\bar{\varsigma}$	$\overline{\overline{\varsigma^{MI}}}$	Compliance	Structural topology	Microstructural topology
0.075	0.4	9855		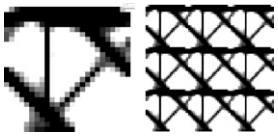
0.09	0.4	7292		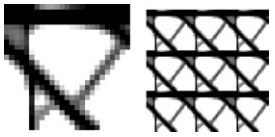
0.12	0.4	5676		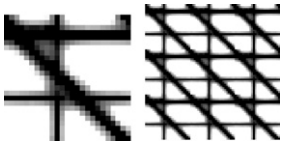
0.18	0.4	3707		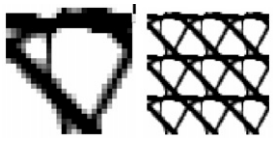
0.25	0.4	2234		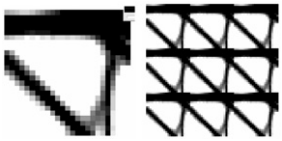

Table 3
Results for varying $\overline{\overline{\varsigma^{MI}}}$

$\bar{\varsigma}$	$\overline{\overline{\varsigma^{MI}}}$	Compliance	Structural topology	Microstructural topology
0.12	0.2	8880		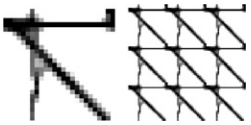
0.12	0.3	6210		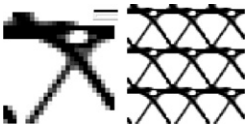
0.12	0.4	5676		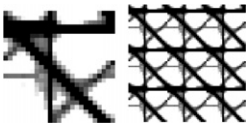
0.12	0.5	5487		

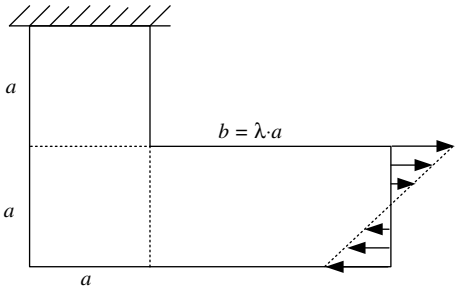

Fig. 7. An L-shaped beam.

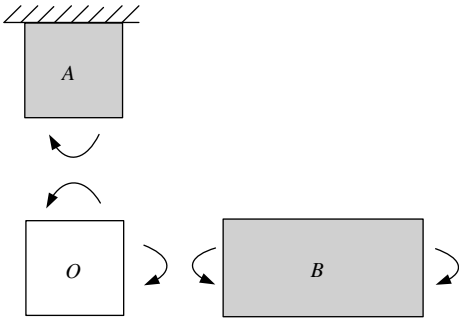

Fig. 8. A decomposition of the L-shaped beam.

5.2. Numerical Example II: a validation of the proposed method

An L-shaped beam in Fig. 7 is considered in this example to validate the proposed method by comparing numerical results with expectations. The upper edge is fixed and a group of loads are applied along the right edge to simulate a moment. For the geometry, $a = 1$ while b is a variable determined by λ. Constraint parameters $\bar{\varsigma}$, $\overline{\overline{\varsigma^{MI}}}$ and $\bar{\gamma}$ are, respectively, fixed to be 0.1, 0.4 and 4.

Note that within the whole structure, material is assumed uniform, but stress conditions could vary considerably, so the design in micro-scale is somehow a multi-objective optimization problem. This example is a good illustration. The L-shaped beam can be divided into three parts as shown in Fig. 8. For bar B, the moments are imposed on the left and right faces resulting in principal deformation in x-direction, and we can therefore expect a larger effective Young's modulus in x-direction for material design. Following similar analysis, the microstructural topology should be stiffer in y-direction for bar A. So the material designs of the two bars seem to be contradictory to some extent. However, they must share the same material microstructure due to the assumption of material uniformity.

This contradiction makes it important the weight between the two bars. λ is, therefore, defined to adjust the weight and three cases are, respectively, considered. If $\lambda = 0$, bar B does not exist and bar A is dominant; If $\lambda = 1$, the weight of bar B is increased; If $\lambda = 2$ and 3, bar B gradually becomes the dominance.

Effective moduli of resulting microstructures are listed in Table 4. Modulus ratio D^H_{11}/D^H_{22} is introduced to indicate the contrast of material arrangement in the two directions where D^H_{pq} ($p, q = 1, 2, 3$ in 2D problem) denotes an element of the modulus matrix. As shown in Table 4, the modulus ratio is increased with increasing λ ($\lambda = 1$ is an exception because in this case the influence of part O in Fig. 8 is greater), which means base material is increasingly arranged to strengthen the porous material in x-direction. This result is perfectly consistent with the above analysis, which again verifies the micro-scale design in a qualitative sense.

Table 4
Results of the L-shaped beam design

$\bar{\varsigma}$	$\overline{\overline{\varsigma^{MI}}}$	λ	Compliance	D_{11}^{H}/D_{22}^{H}	Structural topology	Microstructural topology
0.1	0.4	0	43012	0.55		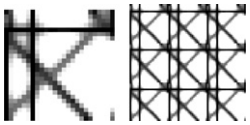
0.1	0.4	1	56958	1.38		
0.1	0.4	2	64345	1.08		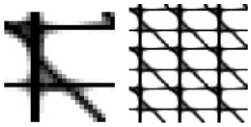
0.1	0.4	3	76590	1.27		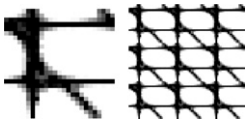

6. Conclusions

This paper presents a concurrent topology design method aimed at searching optimum structure composed of optimum porous anisotropic material.

1. Design variables in two scales are independently defined. Microstructure is no longer restricted to certain specific configurations, which makes it possible to take advantage of various porous/ultra-light materials.
2. In order to achieve clear topologies, PAMP is introduced to penalize porous anisotropic material in macro-scale design, and conventional SIMP is used in micro-scale.
3. Designs in both scales are integrated into one optimization problem and solved concurrently. Constraint parameters $\bar{\varsigma}$, $\overline{\overline{\varsigma^{MI}}}$ and $\bar{\gamma}$ are numerically discussed. Some innovative configurations of macro and micro structures are presented.
4. We strongly underline the uniformity of material microstructure in macro-scale. This assumption will inevitably weaken the benefit derived from the optimum design, but could result in an easier manufacturing process and then illuminate practical applications of the results.

Numerical results illustrate the viability of the method. It is exceptionally interesting to find that for most cases, the optimum microstructures are truss-like structures. These results again demonstrate the superiority of truss-like materials. And these materials can be manufactured by some existing methods for fabricating truss-like materials. It will be an interesting and challenging work to extend this concurrent optimization method to multifunctional application fields (e.g. heat transfer, vibration isolation and mechanical requirements) and 3D problems.

Acknowledgements

The work is supported by National Natural Science Foundation of China (No. 10332010), National Creative Research Team Program of China (No. 10721062) and National Key Basic Research Program of China (973 Program, No. 2006CB601205).

Appendix. Sensitivity analysis

First, we are to write the structural compliance as a summation of elemental compliance

$$C = \sum_{r=1}^{N} C_r = \sum_{r=1}^{N} \mathbf{U}_r^{\mathrm{T}} \cdot \mathbf{K}_r \cdot \mathbf{U}_r \tag{A1}$$

where $\mathbf{U}_r$ and $\mathbf{K}_r$, respectively, denote deformation vector and stiffness matrix of the rth element in macro-scale. Their product equals to the vector of nodal force in the element

$$\mathbf{K}_r \cdot \mathbf{U}_r = \mathbf{F}_r \tag{A2}$$

Note that $\mathbf{F}_r$ is constant for given design variables, so computing the derivation of the two hands with any design variable X will lead to

$$\frac{\partial \mathbf{K}_r}{\partial X} \cdot \mathbf{U}_r + \mathbf{K}_r \cdot \frac{\partial \mathbf{U}_r}{\partial X} = 0 \tag{A3}$$

The derivative of compliance with respect to X is therefore expressed as

$$\frac{\partial C}{\partial X} = \frac{\partial (\sum_{r=1}^{N} \mathbf{U}_r^{\mathrm{T}} \cdot \mathbf{K}_r \cdot \mathbf{U}_r)}{\partial X} = \sum_{r=1}^{N} \frac{\partial (\mathbf{U}_r^{\mathrm{T}} \cdot \mathbf{K}_r \cdot \mathbf{U}_r)}{\partial X} \tag{A4}$$

In order to simplify this expression, expand each item in the right-hand equation as

$$\frac{\partial(\mathbf{U}_r^{\mathrm{T}}\cdot\mathbf{K}_r\cdot\mathbf{U}_r)}{\partial X}=\frac{\partial\mathbf{U}_r^{\mathrm{T}}}{\partial X}\cdot\mathbf{K}_r\cdot\mathbf{U}_r+\mathbf{U}_r^{\mathrm{T}}\cdot\frac{\partial\mathbf{K}_r}{\partial X}\cdot\mathbf{U}_r+\mathbf{U}_r^{\mathrm{T}}\cdot\mathbf{K}_r\cdot\frac{\partial\mathbf{U}_r}{\partial X} \tag{A5}$$

Utilizing Eq. (A3), one will have

$$\frac{\partial(\mathbf{U}_r^{\mathrm{T}}\cdot\mathbf{K}_r\cdot\mathbf{U}_r)}{\partial X}=-\mathbf{U}_r^{\mathrm{T}}\cdot\frac{\partial\mathbf{K}_r}{\partial X}\cdot\mathbf{U}_r \tag{A6}$$

The combination of Eqs. (A4) and (A6) will lead to

$$\begin{aligned}\frac{\partial C}{\partial X}&=-\sum_{r=1}^{N}\mathbf{U}_r^{\mathrm{T}}\cdot\frac{\partial\mathbf{K}_r}{\partial X}\cdot\mathbf{U}_r\\&=-\sum_{r=1}^{N}\mathbf{U}_r^{\mathrm{T}}\cdot\frac{\partial\left(\int_{\Omega_r}\mathbf{B}^{\mathrm{T}}\cdot\mathbf{D}^{\mathrm{MA}}\cdot\mathbf{B}\,\mathrm{d}\Omega\right)}{\partial X}\cdot\mathbf{U}_r\end{aligned} \tag{A7}$$

Now, let us consider the derivative of structural compliance with respect to macro density in the problem with two class design variables. Note that $\mathbf{D}^{\mathrm{MA}}$ can be expressed in the form of Eq. (7), so one can get

$$\begin{aligned}\frac{\partial C}{\partial P_i}&=-\sum_{r=1}^{N}\mathbf{U}_r^{\mathrm{T}}\cdot\frac{\partial\left(\int_{\Omega_r}\mathbf{B}^{\mathrm{T}}\cdot\mathbf{D}^{\mathrm{MA}}\cdot\mathbf{B}\,\mathrm{d}\Omega\right)}{\partial P_i}\cdot\mathbf{U}_r\\&=-\sum_{r=1}^{N}\mathbf{U}_r^{\mathrm{T}}\cdot\frac{\partial\left(\int_{\Omega_r}\mathbf{B}^{\mathrm{T}}\cdot P_r^{\alpha}\cdot\mathbf{D}^{\mathrm{H}}\cdot\mathbf{B}\,\mathrm{d}\Omega\right)}{\partial P_i}\cdot\mathbf{U}_r\\&=-\mathbf{U}_i^{\mathrm{T}}\cdot\int_{\Omega_i}\mathbf{B}^{\mathrm{T}}\cdot\alpha\cdot P_i^{\alpha-1}\cdot\mathbf{D}^{\mathrm{H}}\cdot\mathbf{B}\,\mathrm{d}\Omega\cdot\mathbf{U}_i\\&=-\frac{\alpha}{P_i}\cdot\mathbf{U}_i^{\mathrm{T}}\cdot\int_{\Omega_i}\mathbf{B}^{\mathrm{T}}\cdot P_i^{\alpha}\cdot\mathbf{D}^{\mathrm{H}}\cdot\mathbf{B}\,\mathrm{d}\Omega\cdot\mathbf{U}_i\\&=-\frac{\alpha\cdot C_i}{P_i}\end{aligned} \tag{A8}$$

For the same problem, the derivative of structural compliance with respect to micro density is expressed as

$$\begin{aligned}\frac{\partial C}{\partial\rho_j}&=-\sum_{r=1}^{N}\mathbf{U}_r^{\mathrm{T}}\cdot\frac{\partial\mathbf{K}_r}{\partial\rho_j}\cdot\mathbf{U}_r\\&=-\sum_{r=1}^{N}\mathbf{U}_r^{\mathrm{T}}\cdot\frac{\partial\left(\int_{\Omega_r}\mathbf{B}^{\mathrm{T}}\cdot\mathbf{D}^{\mathrm{MA}}\cdot\mathbf{B}\,\mathrm{d}\Omega\right)}{\partial\rho_j}\cdot\mathbf{U}_r\\&=-\sum_{r=1}^{N}P_r^{\alpha}\cdot\mathbf{U}_r^{\mathrm{T}}\cdot\left(\int_{\Omega_r}\mathbf{B}^{\mathrm{T}}\cdot\frac{\partial\mathbf{D}^{\mathrm{H}}}{\partial\rho_j}\cdot\mathbf{B}\,\mathrm{d}\Omega\right)\cdot\mathbf{U}_r\end{aligned} \tag{A9}$$

References

[1] Ashby MF, Evans AG, Fleck NA, Gibson LJ, Hutchinson JW, Wadley HNG. Metal foams: A design guide. Butterworth Heinemann; 2000.

[2] Wallach JC, Gibson LJ. Mechanical behavior of a three-dimensional truss material. Int J Solids Struct 2001;38:7181–96.

[3] Wang AJ, Mcdowell DL. In-plane stiffness and yield strength of periodic metal honeycombs. J Eng Mater Technol–Trans ASME 2004;126:137–56.

[4] Hayes AM, Wang AJ, Dempsey BM, Mcdowell DL. Mechanics of linear cellular alloys. Mech Mater 2004;36:691–713.

[5] Kooistra GW, Deshpande VS, Wadley HNG. Compressive behavior of age hardenable tetrahedral lattice truss structures made from aluminium. Acta Mater 2004;52:4229–37.

[6] Brittain ST, Sugimura Y, Schueller OJA, Evans AG, Whitesides GM. Fabrication and mechanical performance of a mesoscale space-filling truss system. J Microelectromech Syst 2001;10:113–20.

[7] Cochran JK, Lee KJ, Mcdowell DL, Sanders THB. Multifunctional metallic honeycombs by thermal chemical processing. In: TMS annual meeting. Seattle; 2001.

[8] Cheng GD. On non-smoothness in optimal design of solid elastic plates. Int J Solids Struct 1981;17:795–810.

[9] Bendsoe MP, Kikuchi N. Generating optimal topologies in structural design using homogenization method. Comput Methods Appl Mech Eng 1988;71:197–224.

[10] Deshpande VS, Fleck NA, Ashby MF. Effective properties of the octet-truss lattice material. J Mech Phys Solids 2001;49:1747–69.

[11] Bendsoe MP. Optimal shape design as a material distribution problem. Struct Optim 1989;1:192–202.

[12] Bendsoe MP, Sigmund O. Material interpolation schemes in topology optimization. Arch Appl Mech 1999;69:635–54.

[13] Rodrigues H, Guedes JM, Bendsoe MP. Hierarchical optimization of material and structure. Struct Multidiscip Optim 2002;24:1–10.

[14] Gu S, Lu TJ, Evans AG. On the design of two-dimensional cellular metals for combined heat dissipation and structural load capacity. Int J Heat Mass Trans 2001;44:2163–75.

[15] Hyun S, Torquato S. Optimal and manufacturable two-dimensional, Kagome-like cellular solids. J Mater Res 2002;17:137–44.

[16] Sigmund O. Design of material structures using topology optimization. PhD thesis, Department of Solid Mechanics, Technical University of Denmark, 1994.

[17] Sigmund O. Tailoring materials with prescribed elastic properties. Mech Mater 1995;20:351–68.

[18] Yan J, Cheng GD, Liu ST, Liu L. Comparison of and scale effects on prediction of effective elastic property and shape optimization of truss material with periodic microstructure. Int J Mech Sci 2006;48:400–13.

[19] Haber RB, Jog CS, Bendsoe MP. A new approach to variable-topology shape design using a constraint on perimeter. Struct Optim 1996;11:1–12.

[20] Petersson J, Sigmund O. Slope constrained topology optimization. Int J Numer Meth Eng 1998;41:1417–34.

[21] Zhang WH, Duysinx P. Dual approach using a variant perimeter constraint and efficient sub-iteration scheme for topology optimization. Comput Struct 2003;81:2173–81.

[22] Liu ST, Cheng GD, Gu Y, Zheng XG. Mapping method for sensitivity analysis of composite material property. Struct Multidiscip Optim 2002;24:212–7.